communications earth & environment

ARTICLE

https://doi.org/10.1038/s43247-023-00929-9 OPEN

Atmospheric radiocarbon levels were highly variable during the last deglaciation

Sahra Talamo[1]✉, Michael Friedrich[2]✉, Florian Adolphi[3,4]✉, Bernd Kromer[5], Timothy J. Heaton[6]✉, Silvia Cercatillo[1], Raimund Muscheler[7], Dragana Paleček[1], Enrico Pelloni[1], Laura Tassoni[1], Vladimiro Toniello[8] & Lukas Wacker[9]

Radiocarbon dating provides a key chronological framework for studying past environmental changes. Raw radiocarbon ages measured in samples must be converted to calendar ages using an appropriate calibration curve. Tree-ring datasets provide the gold-standard for developing a precise curve of atmospheric radiocarbon levels over long-time scales. Here, we reconstruct atmospheric radiocarbon levels using a millennium-long section of tree-ring chronology segments that extend into the last glacial period. The samples were obtained from subfossil larch trees recovered from clay quarries at Revine, Italy. Our reconstruction shows higher variations in the amplitude of atmospheric radiocarbon between 18,475 and 17,350 calendar years before the present than that detected in the IntCal20 calibration curve. Comparing the new tree-ring based reconstruction with Beryllium-10 fluxes derived from ice cores, we hypothesise that these variations are driven by solar variability. Our results demonstrate the unique value of sub-decadal radiocarbon sequences derived from glacial tree-ring chronologies.

[1] Department of Chemistry G. Ciamician, Alma Mater Studiorum, University of Bologna Via Selmi 2, Bologna, Italy. [2] Hohenheim Gardens, University of Hohenheim, Stuttgart, Germany. [3] Alfred Wegener Institute, Helmholtz Centre for Polar and Marine Research, Bremerhaven, Germany. [4] Faculty of Geosciences, Bremen University, Bremen, Germany. [5] Institute for Environmental Physics, University of Heidelberg, Heidelberg, Germany. [6] Department of Statistics, School of Mathematics, University of Leeds, Leeds, UK. [7] Quaternary Sciences, Department of Geology, Lund University, Lund, Sweden. [8] Independent researcher, Revine, Italy. [9] Laboratory for Ion Beam Physics, ETH Zurich, Zurich, Switzerland. ✉email: sahra.talamo@unibo.it; michael.friedrich@uni-hohenheim.de; florian.adolphi@awi.de; t.heaton@leeds.ac.uk

Since Willard Libby won the Nobel prize in 1960[1], radiocarbon (^{14}C) has played a revolutionary role in determining the timing and rates of key changes in Earth's climate, our environment, and human society over the last 55,000 years[2–8]. However, as there have been substantial variations in atmospheric $^{14}C/^{12}C$ levels over time, all raw radiocarbon ages need to be calibrated in order to place them on the calendar scale[9–13]. Variations in atmospheric $^{14}C/^{12}C$ ratios, in the following reported as $\Delta^{14}C$, which denotes relative difference to $^{14}C/^{12}C$ at AD 1950 in permille, have occurred due to changes in the rate of ^{14}C production in the upper atmosphere and/or shifts in the carbon cycle. To obtain an accurate and precise calendar age from a fossil sample, we need to know atmospheric $\Delta^{14}C$ at its time of growth. Accurately estimating atmospheric $^{14}C/^{12}C$ variations over time is therefore essential to optimise our use of ^{14}C. The more accurate our knowledge of past $\Delta^{14}C$ levels, the more accurately we can calibrate a ^{14}C measurement to obtain the sample's calendar age.

Improvements in reconstructions of past $\Delta^{14}C$ variations do not however only offer increased accuracy when calibrating radiocarbon determinations. They also provide wider insights into critical Earth and climate system processes. Since ^{14}C production rates vary in response to changes in the strength of the geomagnetic and heliomagnetic fields, understanding past $\Delta^{14}C$ levels and their variations allows reconstruction of the temporal variability of the Earth's magnetic field and of past solar activity[14–16]. The subsequent transport of ^{14}C via the carbon cycle also provides an opportunity to better understand the dynamics of the Earth system, through studying differences in $\Delta^{14}C$ levels across the various carbon cycle reservoirs, from soils to the ocean interior. Carbon exchange between reservoirs and within the ocean affects marine and atmospheric $\Delta^{14}C$ levels[17–19].

Since 1993[9–13], the *INTCAL* working group has been responsible for providing internationally-agreed reconstructions of $\Delta^{14}C$ levels in three principal reservoirs: the Northern Hemispheric (NH) atmosphere[13]; the Southern Hemispheric atmosphere (SH)[20]; and the surface oceans[21]. The most suitable data to produce atmospheric calibration curves are tree-ring ^{14}C measurements dated by dendrochronology. IntCal20, the most recent reconstruction of past NH atmospheric $\Delta^{14}C$levels, uses known-age dendrochronologically dated trees back to c.a. 12,300 cal yr BP[22]. These measurements are extended further using several highly-resolved overlapping ^{14}C tree-ring sequences which, while not dendrochronologically dated, can be almost absolutely linked in terms of calendar age. This provides a highly precise and accurate estimate of $\Delta^{14}C$ levels based upon only tree-ring ^{14}C measurements back to c.a. 13,910 cal yr BP[23].

Further back in time, however, between 14,000 and 55,000 cal yr BP, the IntCal20 estimate of $\Delta^{14}C$ variation is less precise and high-frequency signals cannot currently be resolved. The recovery of NH trees during this glacial period has, to date, been extremely rare. In this critical period of glacial climate, the IntCal20 curve is therefore predominantly based upon combining measurements from a diverse range of additional archives such as speleothems, corals, and lake and marine sediments[13]. These archives have several complications: they are typically sparse, have complex calendar age uncertainties, and frequently do not directly record atmospheric $\Delta^{14}C$. Both speleothems and marine ^{14}C records are depleted in ^{14}C compared to the atmospheric levels via a dead carbon fraction and marine reservoir age, respectively. This depletion is likely to dampen atmospheric ^{14}C variation and may also result in calibration datasets that diverge over time if not appropriately corrected.

Even the Lake Suigetsu record, which contains ^{14}C measurements from terrestrial macrofossils and is used in IntCal20, is not absolutely calendar dated because its original, varve-counted, age scale must be adjusted by matching to ^{14}C features in the Hulu Cave speleothem record[24]. Furthermore, due to their very small size the Lake Suigetsu samples often have large ^{14}C uncertainties. In addition to the limitations of our current ^{14}C archives, the IntCal20 curve prior to 14,000 cal yr BP is also not primarily intended for reconstruction of atmospheric $\Delta^{14}C$ variations. Instead, it is designed for calibration. All the data beyond 14,000 cal yr BP used in IntCal20's construction have uncertainties in their calendar ages. To ensure accurate calibration, this uncertainty needs to be incorporated into the curve. During construction, IntCal20 considers all the possible calendar age placements of its constituent archives and, for each hypothetical placement, creates individual curve realisations representing a plausible $\Delta^{14}C$ history were that calendar age placement correct. While each $\Delta^{14}C$ realisation is wiggly, the precise timing of these wiggles differs by realisation. To enable accurate calibration, IntCal20 must average over the possible calendar age placements of its records. It does this by averaging over all the individual realisations, summarising them by pointwise means and variances. Where calendar age uncertainty in the underlying records is substantial, this averaging results in a mean IntCal20 $\Delta^{14}C$ curve which is smoother than any of its individual realisations[25]. As a consequence of all these factors, it is not possible to resolve high-frequency $\Delta^{14}C$ variation from 14,000 to 55,000 cal yr BP in the IntCal20 NH curve. This currently limits our ability to rigorously test competing scenarios and hypotheses in both archaeological and climate science – particularly regarding the causes of atmospheric $\Delta^{14}C$ variations[26].

The discovery of subfossil trees suitable for the construction of further tree-ring ^{14}C sequences would provide the ideal archives to improve the current lack of precision in the NH atmospheric $\Delta^{14}C$ reconstruction from 14,000 to 55,000 cal yr BP. Due to their annually resolved internal structure, and the direct link between the $\Delta^{14}C$ in tree-ring cellulose and the atmospheric $\Delta^{14}C$, such tree-ring sequences hold the key to resolve high-frequency atmospheric $\Delta^{14}C$ variations and to provide chronologies for sequences involving just a few human generations. Currently, the tree-ring ^{14}C sequences from glacial period that have been measured are known as *floating*. As they do not overlap with the absolutely dated tree-ring dendrochronologies, their absolute calendar ages are unknown[25,27,28]. However, their constituent rings can still be counted to create a relative internal chronology. Even if their absolute ages are not known, this known internal chronology provides important insight into the amplitude of $\Delta^{14}C$ variations over time[29,30].

Typically, these floating trees-ring sequences are incorporated into the IntCal calibration curves by splicing them in alongside other ^{14}C data that have better absolute age controls[25]. However, as explained above, the published IntCal20 curve then averages over their potential absolute calendar age placements. Consequently the IntCal20 mean curve will not reproduce the amplitude of the internal $\Delta^{14}C$ variation observed within any floating tree-ring sequence. This amplitude is critical if we wish to infer potential changes in ^{14}C production rates or changes in the carbon cycle. To reliably estimate this, we must instead consider the $\Delta^{14}C$ variation along the floating tree's relative internal chronology (even if we are not exactly sure, in absolute age terms, when that variation occurred).

Our understanding of potential mechanisms for changes in ^{14}C production rates and the carbon cycle is informed by comparison with other cosmogenic radionuclides, in particular ^{10}Be and ^{36}Cl records stored within ice cores[31–33]. Comparing observed ^{14}C signals with these other cosmogenic radionuclides can be used to align the ice core with ^{14}C timescales[34]; or to help distinguish between changes in the ^{14}C production rate and shifts in the carbon cycle. One disadvantage is that the common production

rate changes of ^{14}C and ^{10}Be vary in a quasi-cyclic fashion on decadal to centennial timescales due to periodic changes in solar activity. Thus, in order to establish a unique link, tree-ring chronologies need to provide relatively long (centennial) time series and possibly prior knowledge of the assumed absolute age window of the records. Another challenge is the different geochemistry of ^{14}C and ^{10}Be: while atmospheric $\Delta^{14}C$ is affected by changes in the carbon cycle, ^{10}Be is affected by deposition changes. Hence, even during strong production rate changes such as during the Laschamps geomagnetic field minimum, seemingly unique matches between ice-core ^{10}Be and tree-ring ^{14}C may be misleading due to apparently large and not well-understood changes in the carbon cycle[35–38].

In order to improve the precision of radiocarbon calibration during the glacial period and to better understand the $\Delta^{14}C$ variations, it is essential to build up further high-precision series of tree-ring-based ^{14}C measurements. For IntCal20, the only NH trees from the deglaciation period, prior to the continuous Central Europe oak and pine dendrochronology, came from Northern Italy and were of a 700-year duration, between 14,000 and 14,700 cal yr BP[31,34]. In Europe, some sub-fossil trees of glacial age were deposited in sediments of river valleys, such as the Po plain and quarries in Italy, and in other glacial deposits. Here we demonstrate the potential of subfossil larch trees from North-East Italy at the Revine site (Venetian Prealps)[39,40], to provide more detailed reconstructions of $\Delta^{14}C$ further into the glacial. We present the first 1000-year-long section of tree-ring chronology segments, and corresponding sub-decadal ^{14}C-series, covering the period from c.a. 18,475-17,350 cal yr BP in Heinrich Stadial 1 (HS-1) (Fig. 1). Our data provide a higher-resolution archive of $\Delta^{14}C$ variations during HS-1 than achievable with IntCal20, with patterns associated with changes in solar activity[41–43].

Results

Dendrochronological results. The dendrochronological analysis of 33 larch samples (*Larix decidua* Mill.) provided 25 tree-ring series, which could be combined into tree-ring chronologies. Based on the statistical and visual agreement (Supplementary Table 1a–d), 12 tree-ring series were combined to generate the Revine group 1 (Gr. 1) chronology (336 years; average $t_{B\&P}$: 8.54) (Supplementary Fig. 1). Three other tree-ring series were combined together to create the Revine Gr.3 chronology (296 years; average $t_{B\&P}$: 8.4) (Supplementary Fig. 2). Comparisons between chronologies Revine Gr.1 and Gr.3 revealed good visual and statistical correlations ($T_{B\&P}$: 5.6; Glk 63%; $P > 99\%$) (Supplementary Fig. 3) that could be additionally affirmed by ^{14}C-series comparisons on both groups. The combined chronology (Revine Gr.1/3) spans 429 years. Two tree-ring series were combined into the Revine Gr.4 chronology (260 years; average $t_{B\&P}$: 7,1) (Supplementary Fig. 4) and another four larch series were combined to form the Revine Gr.2 chronology (286 years; average $t_{B\&P}$: 7,1) (Supplementary Fig. 5).

In almost all cases, the trees consisted of trunks or stumps without branches and sapwood, and the outermost ring or bark was not preserved. Therefore, the exact year of death of the trees cannot be determined. The larch trees show an average ring width of 0.9 mm (Gr. 1), 0.98 mm (Gr. 2), 0.69 mm (Gr. 3), and 0.84 mm (Gr. 4), which is comparable to modern sites at the alpine altitudinal timberline at ca. 2000 m asl. The frequent occurrence of partial and total absent rings, especially in the Revine Gr. 1 chronology, is associated with the influence of larch moth infestation, which regularly leads to extremely low growth every 7–11 years in some trees. In Revine Gr. 1, 75% of the trees show locally absent rings. The procedure described for recent and late Holocene larch chronologies to identify larch budmoth years of infestation and conceivable totally absent tree rings using a non-host species chronology as a ref. [44] is not possible for this dataset. However, the successful cross-matching of the Revine Gr. 1 chronology with the Revine Gr. 3 chronology, whose trees are much less affected by the pest and do not show any absent rings, allows an additional validation of the chronologies, as it covers the full critical period (203 years) of Gr. 3. The influence of larch budmoth outbreaks is minor in Gr. 2, and totally absent in Gr. 4. Hence, the possibility of further unidentified tree rings in the chronologies is extremely unlikely. Chronologies Revine Gr. 1/3, Gr. 2, and Gr. 4 represent secure and robust floating tree-ring chronologies that are the solid basis for our high-resolution ^{14}C series described in this work (Supplementary Table 2).

The three Revine chronologies (Gr. 1/3, Gr. 2, and Gr. 4) do not cross-date dendrochronologically, indicating that the trees likely grew during different time intervals, also confirmed by the later ^{14}C analyses. From ^{14}C data, a short overlap of 51 years between Gr. 4 and Gr. 2 is possible, which coincides with a visual tentative match of the tree-ring curves. This overlap cannot be

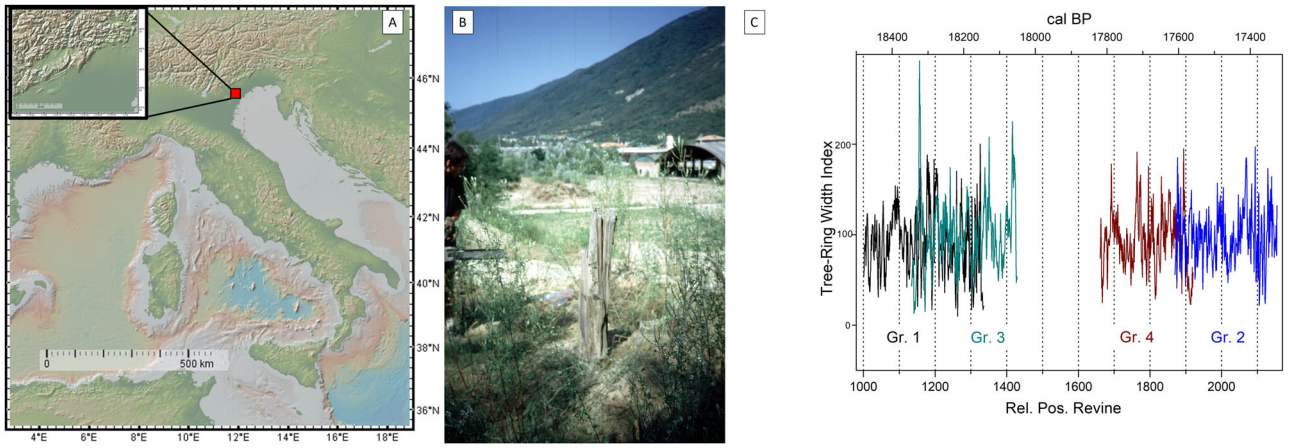

Fig. 1 Revine Trees, location and chronologies. A map showing the location of Revine (red square) (base map from GeoMappApp (www.geomapapp.org); **B** Revine trees collected in 1995 by B.K. field campaign (The photo is taken by B.K. co-author of the paper, and under his copyright); **C** Ring width index chronologies of Revine groups 1, 3, 2 and 4 on its relative Revine timescale. The relative positions resp. the approximately absolute ages of the tree-ring series are based on the $\Delta^{14}C$ comparisons. Gr.1 and Gr.3 are matched dendrochronologically ($t_{Baillie\&Pilcher}$: 5,1). Gr. 2 and Gr. 4 overlap only very slightly and they do not show any obvious statistical significant match. Their tentative position is based on a multi-step argumentation line of $\Delta^{14}C$ comparisons, ^{10}Be-$\Delta^{14}C$ comparisons and the statistically non-significant visual match of the tree-ring series.

statistically validated because of its short duration and low replication, but can be supported by the link to ^{10}Be, as discussed below. We therefore further use the position of this tentative link, which lies well within the uncertainty range of the ^{14}C-data. Comparison with existing ^{14}C data from the speleothems of Hulu Cave[36,45] and macrofossils of Lake Suigetsu[24] indicate that the 3 chronologies cover a period of ca. 1200 calendar years (18,475–17,325 cal yr BP), albeit with a gap of c.a. 200 calendar years (from c.a. 18,050 to 17,850 cal yr BP) between the youngest ring of Gr. 1/3 and the oldest ring of Gr. 4.

^{14}C results and link to IntCal20 raw data. One hundred and ten blocks (each consisting of three annual rings) at mostly decadal spacing were taken from the entire length of the Revine chronologies for radiocarbon age determination. The chronologies fall in a ^{14}C age range between 15,250 and 14,180 ^{14}C BP (Supplementary Table 2). While the absolute calendar age of each distinct Revine chronology is unknown, the internal chronology within each of the three tree-ring groupings (Revine Gr. 1/3; Gr. 2; and Gr. 4) is due to dendrochronological ring counting. Reconstructing the atmospheric Δ^{14}C levels seen within the Revine trees over the course of their exact internal chronologies allows us to obtain unique insight into the amplitude of Δ^{14}C variation during HS-1. Furthermore, we can obtain relatively precise absolute calendar age positioning for each Revine Chronologies by comparison with existing ^{14}C measurements from Hulu Cave[36,45] and Lake Suigetsu[24] for which independent estimates of calendar age have been obtained by the U-Th (uranium-thorium) method and varve counting respectively (see Methods for details). This comparison suggests that the most likely calendar dates (the posterior marginal mode) for the innermost ring of the tree-ring chronologies are 18,475 cal yr BP (±35 cal yrs) for Revine Gr. 1/3; 17,605 cal yr BP (±50 cal yrs) for Revine Gr. 2; and 17,830 (±55 cal yrs) for Revine Gr. 4. These calendar age placements are shown in Fig. 2 (alongside the Hulu and Suigetsu ^{14}C measurements).

Revine Gr. 1/3 documents in detail a strong decline in ^{14}C ages (rise in Δ^{14}C) between 18,300 and 18,100 cal yr BP. This ^{14}C age decline is seen more clearly within the Revine Gr. 1/3 tree-ring sequence than in the smoothed and indirect Hulu and Lake Suigetsu ^{14}C data. The ^{14}C age inversion apparent in IntCal20 around 18,400 cal yr BP appears to be artefact of systematic differences between the two raw data sets of IntCal20 rather than a genuine atmospheric feature. A similar discrepancy is evident between 17,600 and 17,300 cal yr BP in the IntCal20 raw data. In general, our tree-ring Revine data appear to confirm the sequence of the Hulu ^{14}C data but with a resolution that is 10 times greater and with a reduced level of smoothing.

Figure 3 shows the reconstruction of Δ^{14}C based on the Revine trees alone (located at their most likely calendar ages according to the comparison with the Hulu and Suigetsu ^{14}C data). This reconstruction uses the same spline methodology as for the dendrodated tree-ring section of IntCal20[21]. Knots have been placed every 5 cal yrs. The amplitude of the Δ^{14}C variations within the Revine trees appear to be of greater magnitude ($\delta\Delta^{14}$C 45‰) than those observed within the Holocene ($\delta\Delta^{14}$C 20 to 35‰– see Supplementary Fig. 6 which presents the three periods in the Holocene with the greatest Δ^{14}C variation). This increase in Δ^{14}Cvariation during HS-1 is perhaps due to differences in the carbon cycle (e.g., rate of exchange between ocean and atmosphere, internal mixing of Southern Atlantic Ocean)[42,43].

^{10}Be link to ice core scale GICC05. We compare our Revine ^{14}C-data, placed at their posterior modal calendar ages, to ice-core ^{10}Be records. In the case of Revine, the tree-ring records are relatively short and record the quasi-cyclic ^{14}C-variations caused by the solar DeVries (~200 years) and Gleissberg (~90 years) cycles which occur throughout large parts of the Last Glacial Maximum[46]. This leads to many acceptably good matches between the ice-core and tree-ring data but limits the possibility to use the Revine trees to constrain the ice core timescale. In addition, the Greenland ice core timescale GICC05[47] has been shown to systematically deviate from the radiocarbon timescale during the glacial over long periods, with the greatest change in the inferred difference between the ice core and ^{14}C timescale occurring between Greenland Interstadial 1 and ~22,000 cal yr BP[48]. Linearly interpolating between the latest estimate of the timescale difference of approx. zero years around 13,000 cal yr BP and 375 years at 22,000 cal yr BP[48,49] implies an offset of around 190 years at 18,000 cal yr BP. We note, however, that the older tie-point is particularly uncertain (68.2% probability interval from 75 to 625 years). Once we include the ice-core layer counting

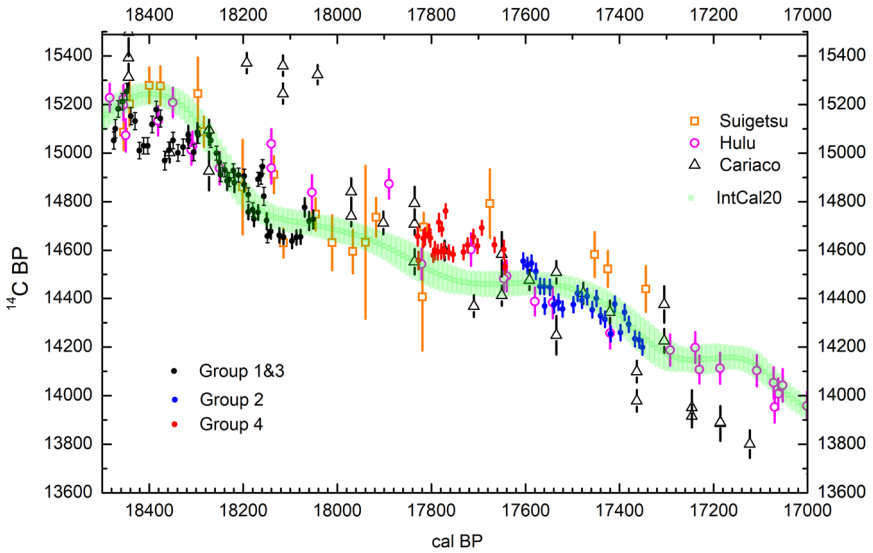

Fig. 2 Revine tree-ring ^{14}C data. The ^{14}C dates of Revine groups and their respective calendar ages in comparison with ^{14}C measurements from Hulu Cave (purple open circle), Lake Suigetsu (orange open square), the marine foraminifera from Cariaco basin (black triangles) and the IntCal20 calibration curve (green dots)[68], using the MCMC scheme. All the dates are plotted with 1σ error bars.

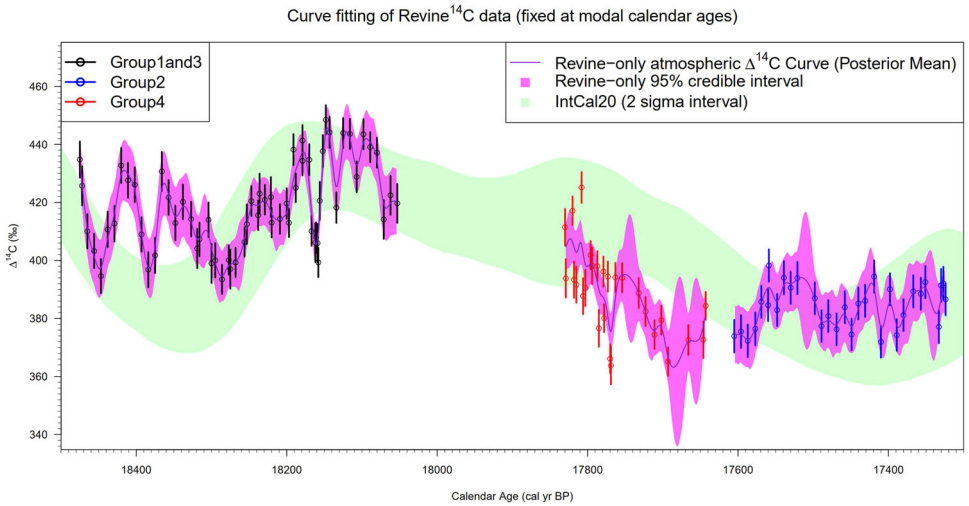

Fig. 3 Reconstruction of $\Delta^{14}C$. Atmospheric ^{14}C reconstruction based on Revine ^{14}C tree-ring sequences located at their most likely (marginal posterior mode) calendar ages compared to IntCal20 estimate (green shape). The Revine observations are plotted with 1σ error bars, while the IntCal and Revine curves show 95% (or 2σ) probability intervals.

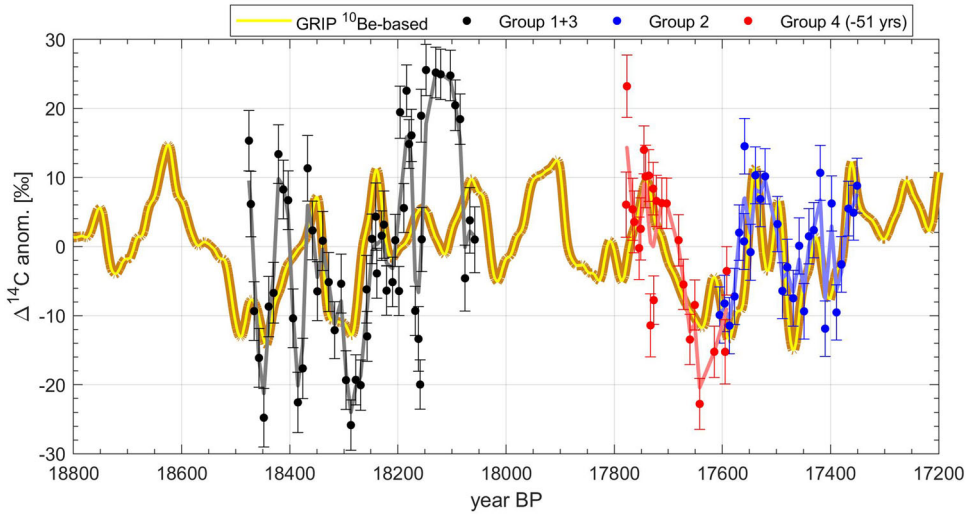

Fig. 4 Absolute ages of the tree-ring data. Comparison of the 3 floating tree-ring chronologies (coloured symbols, plotted with 1σ error bars) to modelled $\Delta^{14}C$ based on ^{10}Be-fluxes from the GRIP ice core (yellow line)[46]. The absolute ages of the tree-ring data are inferred by $^{14}C/^{12}C$ comparison. The $\Delta^{14}C$ is shown as the anomaly from the mean of each chronology. The ice-core data are shown on the GICC05 timescale shifted by +190 years[48,49] and high-pass filtered with a cutoff-period of 1000 years.

errors in between the tie-points of 211 years between 13,000 and 18,000 cal yr BP, and 180 years between 18,000 and 22,000 cal yr BP, it becomes clear that the ice cores cannot be used to provide strong (independent) constraints on the precise calendar ages of the Revine trees during this period.

Nonetheless, the ^{10}Be record is still able to provide useful inferential support. Figure 4 shows the comparison between ice-core ^{10}Be and the Revine tree-ring ^{14}C data. We modelled $\Delta^{14}C$-variations from ^{10}Be using a box-diffusion carbon cycle model[50] under a constant carbon cycle with reduced air-sea gas-exchange and ocean internal mixing compared to preindustrial[48]. As discussed above, we shifted the ice-core timescale by +190 years to account for the previously inferred differences between the ice core timescales GICC05 and IntCal[48,49]. Especially for Gr. 2 (blue symbols in Fig. 4), there is a good match between ice-core ^{10}Be and tree-ring ^{14}C, lending support to the proposed ages for the tree-ring chronology and the ice-core timescale adjustment. Gr. 4 agrees with the ^{10}Be best when shifted 50 calendar years younger than the posterior marginal modal calendar age (17,830 cal yr BP) that is obtained when using the Hulu cave and Lake Suigetsu ^{14}C data. This revised calendar age placement of Gr. 4 is, however, well within the calendar uncertainty (±55 yr) of the match and also supported by a tentative dendrochronological match between Gr. 4 and Gr. 2. The combined Gr. 1/3 data show co-variability between 18,200 and 18,400 cal yr BP lending support to their relative alignment. However, the tree-ring ^{14}C-data exhibits $\Delta^{14}C$ variations of greater amplitude than those inferred from ice-core ^{10}Be. This is possibly due to the lower resolution of the ^{10}Be-data, which, in this period, is an average of around 25 cal yrs. This means that it cannot capture some of the high-frequency changes resolved by the tree-ring data. Higher-resolution ^{10}Be-data could help to resolve this and enable a more robust link between tree-rings and ice cores. Nonetheless, this comparison lends support to the proposed difference between ice-core and radiocarbon time-scales during the glacial, as well as to the inferred calendar ages for the tree-rings.

Generally, ^{14}C and ^{10}Be are covariant in the solar variability time spectrum, except for about one century around 18,100 cal yr BP. Here, ^{14}C is increasing in the atmosphere, most probably caused by a reduction in ^{14}C uptake of the Atlantic Ocean mixed layer at the onset of HS-1. A reduction of AMOC strength at the onset of HS-1 is indicated by an increase of $^{231}Pa/^{230}Th$ ratio in ocean sediments of the western deep Atlantic[51]. Also, a sedimentary terrestrial high-resolution record from Southern Iberia reveals centennial subphases of HS-1, starting cold and arid at ca. 18,400 cal yr BP[52]. However, only the tree-ring record can provide decadal resolution in ^{14}C to study the effect of a weakening AMOC on the carbon cycle on decadal time scales.

Discussion and conclusion

The temporal alignment suggested by comparison to other absolutely-dated ^{14}C records and ^{10}Be links, resulting in a sequence without major gaps, confirms the existence of a well-established larch forest in the Alpine region during HS-1, i.e., by the initial Revine site study[39]. In the southern Alpine region, other fossil wood dated back to 18,300 cal yr BP is found in Lago Piccolo di Avigliana (353 m a.s.l). Together with pollen evidence (e.g., Lago di Viverone, 220 m a.s.l., Torfsee, 270 m a.s.l.,[53]), it suggests that larch was already present in the lowlands when deglaciation started[53–55]. The larch tree finds at Revine together with abundant macrofossils and pollen findings in different regions of northern Italy[56,57] indicate that larch pioneer forests may have been widespread in the southern alpine region during HS-1 and that larch forest-steppe persisted throughout GS-2[58].

The onset and the duration of the larch forest documented at Revine is synchronous with the end of the Alpine Late Glacial Maximum and the Alpine ice retreat at 19,000-17,500 cal yr BP. This is consistent with global climate warming[59] and increased drought in the Mediterranean[60,61]. Here we have demonstrated the advantage of tree-ring ^{14}C data sets, where the decadal temporal resolution is three to ten times higher than that of the Suigetsu and Hulu archives, and the ^{14}C uncertainty is reduced by a factor of two to three. We also note that in the period covered by our trees, the Hulu and Suigetsu ^{14}C data often appear somewhat offset from one another with the IntCal20 curve falling in between. Our ^{14}C data set appears to follow the Hulu data more closely than Suigetsu. Hence, we see an important role for our data in future IntCal calibration data during this time range as well as a possible need for minor revisions to the Suigetsu calendar timescale.

This work clearly shows the strength of the combined studies of dendrochronology, radiocarbon dating, and ^{10}Be to develop new floating tree-ring width chronologies and high-resolution ^{14}C-data sequences from sub-fossil trees grown during the most recent glacial period. As already outlined above, fieldwork is ongoing in the Mediterranean area. Newly found trees, together with those already existing, will provide ^{14}C data sets of sub-decadal temporal resolution and high ^{14}C precision in various time intervals. The findings document intervals of favourable conditions of forest growth, contributing strongly to local paleoclimate reconstruction during the last glacial period.

Material and methods

The subfossil larch trees of Revine. The paleoenvironmental context of the deposits with subfossil wood stems in the clay quarry of Revine was initially studied between 1972 and 1976[39,40]. At that time, 70 subfossil larch (*Larix decidua* Mill.) tree stumps and trunks were found 'in situ' and described. The trees grew during the deglaciation at the edge of the Glacial main moraine rim at a glacial lake and were gradually covered by fine-grained colluvial deposits, which allowed for excellent preservation. By our own fieldwork and investigations at museums, universities and private collections since 1994, 34 individual larch (*Larix decidua* Mill.) and two individual elder trees (Alnus spec.) of the same site in Revine were collected. Sixteen of these trees could be reliably assigned to the original logs sampled in 1976 and thus embedded in the stratigraphy established by Casadoro[39]. Five logs were documented and resampled during our own fieldwork in the no longer used clay pit. The dendrochronological analyses were carried out at the University of Hohenheim, and 3 chronologies of 429, 296, and 286 rings (which were not connected to one another dendrochronologically) could be constructed. Initial radiocarbon analysis on some single tree sections gave the first insight into the variation of ^{14}C in the period of Heinrich Stadial-1 (HS-1)[41]. Then high-resolution (sub-decadal) ^{14}C data sets were obtained covering in total almost one millennium. Subsequently, these results were compared to ^{10}Be in Greenland Ice cores.

Dendrochronological analysis. The clean cross section at surfaces of the subfossil trees were cut with razor blades to enable precise visual identification of the ring boundaries using a microscope. Measurements of the annual growth widths on multiple radii per tree were made using a LINTAB measurement device of RinnTech (Heidelberg, Germany) with an accuracy of 0.01 mm and the software TSAPWin (Version 4.87)[62]. Cross-dating, chronology building and data verification were performed with software program TSAPWin[62]. Cross-dating measurements were compared using standard dendrochronological cross-dating statistics: Student's t-values based on cross-correlation coefficients (r) between the detrended measurement series ($t_{B\&P}$)[63] and a sign test (GLK %) with its significance level (p)[64]. Programs that support chronology building (COFECHA[63,65]) were not useful here, as they give very contradictory results for larch trees with rhythmically occurring narrow rings, which are typical when tree are affected by the larch bud moth. In order to ensure the identification of all rings, even the partially absent ones, we prepared the entire surface on several discs per tree and measured a large number of radii, including in areas of reaction wood or root attachments, where remnants of partially absent rings are often still detectable.

Revine samples preparation and ^{14}C dating. From the four tree-ring chronologies of Revine, we selected tree specimens with well-preserved wood. A series of sub-samples of 3 rings each (25 to 500 mg) was cut in the Hohenheim tree-ring laboratory and sent to the BRAVHO radiocarbon laboratory at the University of Bologna, Italy, for extraction of cellulose. For ^{14}C measurements, every third 3-ring sample (every 9 years) were selected. Most of the samples were pretreated using the BABAB method[66]. Samples of low preservation, resp. very low initial dry weight had to be pretreated by ABAB[66]. Until the end of 2021, the cellulose samples were graphitized at the Radiocarbon laboratory of ETH Zurich. From then on, they were graphitized at BRAVHO, using an AGE 3 system. All samples were measured by AMS at ETH Zurich. The results are listed in Supplementary Table 2.

Estimation of absolute calendar ages for the three Revine ^{14}C chronologies. Each of the three Revine tree-ring groupings was considered to have an unknown calendar age for its oldest measured ring (denoted $S_{1/3}$, S_2, and S_4 respectively). These values were estimated via a Bayesian errors-in-variables Markov Chain Monte Carlo (MCMC) scheme based upon the approach used to incorporate the floating tree-ring sequences into IntCal20[25]. The Revine ^{14}C measurements were combined with ^{14}C observations from between 19,000 and 17,000 cal yr BP provided by the H82 and MSL Hulu Cave speleothems, and the ^{14}C observations from the macrofossils from Lake Suigetsu. While the absolute calendar ages θ_i of the Hulu and Lake Suigetsu

^{14}C measurements are themselves uncertain, estimates T_i are available via U/Th and an adjusted varve count respectively. Given the age of the oldest ring in a Revine tree-ring group, the entire chronology for that particular grouping becomes known precisely due to the internal ring-counts. Within our MCMC scheme, the common atmospheric level of Δ^{14}C was modelled as a Bayesian cubic spline (placing knots every 5 cal yrs) with unknown coefficients β and an unknown smoothing parameter λ. Fit to the ^{14}C data was assessed in the F^{14}C domain where observational uncertainties are symmetric.

Intuitively, the MCMC scheme aimed to find plausible calendar age placements for all the ^{14}C measurements within the Revine, Hulu and Suigetsu records simultaneously (while respecting the complex calendar age covariance structure within the Hulu and Suigetsu observations, and the known internal ring counts of the three Revine groupings). These calendar age placements are obtained based on the principle that the ^{14}C measurements from all the records arise from a common and shared atmosphere, albeit in the case of the Hulu speleothem, the observed Δ^{14}C is offset from the atmosphere by its dead carbon fraction (DCF). It is critical to locate all the Revine groupings on the calendar scale simultaneously (rather than to wiggle match each Revine sequence separately) since every group provides information on the atmospheric levels of ^{14}C/^{12}C (and on the DCF of Hulu), and hence, informs the placement of each other.

Metropolis-within-Gibbs was implemented to alternate between updates to the spline coefficients β (that represent the joint atmospheric estimate of Δ^{14}C)[67], updates to the smoothing parameter λ, and updates to the true calendar ages of the various ^{14}C measurements – both for the comparison Hulu and Lake Suigetsu observations; and the three Revine groupings. We modelled the mean DCF within the Hulu Cave speleothems as unknown, with a prior value of $N(480, 8^2)$ ^{14}C yrs. This was selected based upon investigation into the observed offset between Hulu Cave ^{14}C measurements and contemporaneous ^{14}C measurements from dendro-dated trees[25] between 14,000 and 10,000 cal yr BP. This means DCF value was also updated within our MCMC scheme. Additionally, we placed a further level of independent variation of 50 ^{14}C yrs on the Hulu DCF (at 1σ) to model any temporal DCF variation around the mean level. This choice of ±50 ^{14}C yrs was again based on investigation into the variability of Hulu's ^{14}C offset to dendro-dated tree-ring measurements. Uninformative priors were placed on both the smoothing parameter λ, and on the starting calendar ages ($S_{1/3}$, S_2, and S_4) of the Revine groupings.

The sampler was run for 250,000 iterations with the addition of parallel tempering to improve chain mixing. The first 125,000 iterations were discarded as burn-in. This provided complete posterior calendar age estimates for each of $S_{1/3}$, S_2, and S_4. The posterior mean for the calendar age of the oldest ring in Revine Gr. 1/3 was 18,450 ± 34 cal yrs (1σ); for Gr. 2 it was 17,588 ± 49 cal yrs; for Gr. 4 it was 17,849 ± 54 cal yrs. However, rather than using the mean values, for our investigation into the amplitude of the atmospheric ^{14}C/^{12}C we chose to fix each Revine chronology at its marginal posterior mode calendar age. These modal ages represent the most-likely individual calendar ages for the sequences according to our modelling above using the Hulu and Lake Suigetsu ^{14}C records. For Revine Gr. 1/3 this was 18,475 cal yr BP; for Gr. 2 it was 17,605 cal yr BP; and for Gr. 4 it was 17,830 cal yr BP. These calendar age placements are shown in Figs. 2 and 3. For Gr. 4 a shift by 51 years to younger ages appears possible, as discussed below, and used when creating the Revine-only atmospheric Δ^{14}C curve in Fig. 3.

Data availability

The radiocarbon data generated in this study are available in the Supplementary Information. The Supplementary Tables 1 and 2 are also available at https://figshare.com/articles/dataset/Untitled_Item_strong_Supplementary_Table_1a-d_strong_/23642169?file=41486265 and https://figshare.com/articles/dataset/Suppl_table_2_xlsx/23541285, respectively. The Berylium-10 data from GRIP ice core present in Fig. 4 can be found in Supplementary table of https://www.nature.com/articles/ngeo2225#Sec4. The IntCal20 data (including all raw data, shown in Figs. 2 and 3) are available at https://www.intcal.org.

Received: 15 January 2023; Accepted: 11 July 2023;
Published online: 22 July 2023

References

1. Libby, W. F. Radiocarbon dating. *Science* **133**, 621–629 (1961).
2. Friedrich, W. L. et al. Santorini Eruption Radiocarbon Dated to 1627–1600 B.C. *Science* **312**, 548 (2006).
3. Talamo, S. et al. A 41,500 year-old decorated ivory pendant from Stajnia cave (Poland). *Scientific Reports* **11**, 22078 (2021).
4. Hublin, J.-J. et al. Initial upper palaeolithic homo sapiens from Bacho Kiro cave, Bulgaria. *Nature* **581**, 299–302 (2020).
5. Di Maida, G., Mannino, M. A., Krause-Kyora, B., Jensen, T. Z. T. & Talamo, S. Radiocarbon dating and isotope analysis on the purported Aurignacian skeletal remains from Fontana Nuova (Ragusa, Italy). *PLoS ONE* **14**, e0213173 (2019).
6. Perri, A. R. et al. Detecting hidden diets and disease: zoonotic parasites and fish consumption in Mesolithic Ireland. *J. Archaeol. Sci.* **97**, 137–146 (2018).
7. Rudaya, N., Vasiliev, S., Viola, B., Talamo, S. & Markin, S. Palaeoenvironments during the period of the Neanderthals settlement in Chagyrskaya cave (Altai Mountains, Russia). *Palaeogeography, Palaeoclimatology, Palaeoecology* **467**, https://doi.org/10.1016/j.palaeo.2015.12.007 (2017).
8. Schaub, M. et al. Lateglacial environmental variability from Swiss tree rings. *Quart. Sci. Rev.* **27**, 29–41 (2008).
9. Stuiver, M. et al. INTCAL98 radiocarbon age calibration. *Radiocarbon* **40**, 1041–1083 (1998).
10. Reimer, P. J. et al. INTCAL04 terrestrial radiocarbon age calibration, 0–26 cal kyr BP. *Radiocarbon* **46**, 1029–1058 (2004).
11. Reimer, P. J. et al. IntCal09 and Marine09 radiocarbon age calibration curves, 0 – 50 cal kBP. *Radiocarbon* **51**, 1111–1150 (2009).
12. Reimer, P. J. et al. IntCal13 and marine13 radiocarbon age calibration curves 0–50,000 years cal BP. *Radiocarbon* **55**, 1869–1887 (2013).
13. Reimer, P. J. et al. The IntCal20 Northern hemisphere radiocarbon age calibration curve (0–55 cal kbp). *Radiocarbon* **62**, 725–757 (2020).
14. Bucha, V. & Neustupný, E. Changes of the earth's magnetic field and radiocarbon dating. *Nature* **215**, 261–263 (1967).
15. Solanki, S. K., Usoskin, I. G., Kromer, B., Schussler, M. & Beer, J. Unusual activity of the Sun during recent decades compared to the previous 11,000 years. *Nature* **431**, 1084–1087, http://www.nature.com/nature/journal/v431/n7012/suppinfo/nature02995_S1.html (2004).
16. Reimer, P. J. Solar physics: spots from rings. *Nature* **431**, 1047–1048 (2004).
17. Warren, B. J. et al. Extremely large variations of atmospheric ^{14}C concentration during the last Glacial period. *Science* **292**, 2453–2458 (2001).
18. Hughen, K. A. et al. ^{14}C Activity and global carbon cycle changes over the past 50,000 years. *Science* **303**, 202–207 (2004).
19. Heaton, T. J. et al. Radiocarbon: a key tracer for studying Earth's dynamo, climate system, carbon cycle, and Sun. *Science* **374**, eabd7096 (2021).
20. Hogg, A. G. et al. SHCal20 southern hemisphere calibration, 0–55,000 years Cal BP. *Radiocarbon*, 1–20, https://doi.org/10.1017/RDC.2020.59 (2020).
21. Heaton, T. J. et al. Marine20—The marine radiocarbon age calibration curve (0–55,000 Cal Bp). *Radiocarbon*, 1–42, https://doi.org/10.1017/RDC.2020.68 (2020).
22. Kromer, B. et al. Late Glacial ^{14}C ages from a floating 1382-ring pine chronology. *Radiocarbon* **46**, 1203–1209 (2004).
23. Bayliss, A. et al. IntCal20 tree rings: an archaeological swot analysis. *Radiocarbon*, 1–34, https://doi.org/10.1017/RDC.2020.77 (2020).
24. Bronk Ramsey, C. et al. Reanalysis of the atmospheric radiocarbon calibration record from lake Suigetsu, Japan. *Radiocarbon*, 1–11, https://doi.org/10.1017/RDC.2020.18 (2020).
25. Heaton, T. J. et al. The IntCal20 approach to radiocarbon calibration curve construction: a new methodology using Bayesian splines and errors-in-variables. *Radiocarbon* **62**, 821–863 (2020).

26. Dutta, K. Sun, ocean, nuclear bombs, and fossil fuels: radiocarbon variations and implications for high-resolution dating. *Ann. Rev. Earth Planet. Sci.* **44**, 239–275 (2016).
27. Friedrich, M. et al. The 12,460-Year Hohenheim oak and pine tree-ring chronology from central Europe - a unique annual record for radiocarbon calibration and paleoenvironment Reconstructions. *Radiocarbon* **46**, 1111–1122 (2004).
28. Reinig, F. et al. Illuminating IntCal during the Younger Dryas. *Radiocarbon*, 1-7, https://doi.org/10.1017/RDC.2020.15 (2020).
29. Hogg, A. G. et al. Advances and limitations in establishing a contiguous high-resolution atmospheric radiocarbon record derived from subfossil kauri tree rings for the interval 60–27 cal kyr BP. *Quat. Geochronol.* **68**, 101251 (2022).
30. Lorrey, A. M. et al. The scientific value and potential of New Zealand swamp kauri. *Quat. Sci. Rev.* **183**, 124–139 (2018).
31. Adolphi, F. et al. Radiocarbon calibration uncertainties during the last deglaciation: insights from new floating tree-ring chronologies. *Quat. Sci. Rev.* **170**, 98–108 (2017).
32. Beer, J. et al. Cosmogenic nuclides during Isotope Stages 2 and 3. *Quat. Sci. Rev.* **21**, 1129–1139 (2002).
33. Muscheler, R., Beer, J., Kubik, P. W. & Synal, H.-A. Geomagnetic field intensity during the last 60,000 years based on ^{10}Be and ^{36}Cl from the Summit ice cores and 14C. *Quat. Sci. Rev.* **24**, 1849–1860 (2005).
34. Muscheler, R. et al. Testing and improving the IntCal20 calibration curve with independent records. *Radiocarbon* 1–16, https://doi.org/10.1017/RDC.2020.54 (2020).
35. Muscheler, R., Adolphi, F. & Svensson, A. Challenges in ^{14}C dating towards the limit of the method inferred from anchoring a floating tree ring radiocarbon chronology to ice core records around the Laschamp geomagnetic field minimum. *Earth Planet. Sci. Lett.* **394**, 209–215 (2014).
36. Cheng, H. et al. Atmospheric ^{14}C/^{12}C changes during the last glacial period from Hulu Cave. *Science* **362**, 1293 (2018).
37. Raisbeck, G. M., Yiou, F., Jouzel, J. & Stocker, T. F. Direct north-south synchronization of abrupt climate change record in ice cores using beryllium-10. *Clim. Past* **3**, 541–547 (2007).
38. Cooper, A. et al. A global environmental crisis 42,000 years ago. *Science* **371**, 811 (2021).
39. Casadoro, G. Un deposito tardowuermiano con tronchi subfossili alle fornaci di Revine (Treviso). *Boli. Comi. GIac. It.* **24**, 22–63 (1976).
40. Corona, E. Una curva trisecolare per larice del Dryas Antico. *Dendrochronologia* **2**, 83–89 (1984).
41. Kromer, B., Spurk, M., Remmele, S., Barbetti, M. & Joniello, V. Segments of atmospheric 14C change as derived from late glacial and early holocene floating tree-ring series. *Radiocarbon* **40**, 351–358 (1997).
42. Yu, J. et al. Millennial and centennial CO_2 release from the Southern Ocean during the last deglaciation. *Nat. Geosci.* **15**, 293–299 (2022).
43. Skinner, L. C. et al. Atlantic ocean ventilation changes across the last deglaciation and their carbon cycle implications. *Paleoceanogr. Paleoclimatol.* **36**, e2020PA004074 (2021).
44. Nola, P., Morales, M., Motta, R. & Villalba, R. The role of larch budmoth (Zeiraphera diniana Gn.) on forest succession in a larch (Larix decidua Mill.) and Swiss stone pine (Pinus cembra L.) stand in the Susa Valley (Piedmont, Italy). *Trees* **20**, 371–382 (2006).
45. Southon, J., Noronha, A. L., Cheng, H., Edwards, R. L. & Wang, Y. A high-resolution record of atmospheric ^{14}C based on Hulu Cave speleothem H82. *Quat. Sci. Rev.* **33**, 32–41 (2012).
46. Adolphi, F. et al. Persistent link between solar activity and Greenland climate during the Last Glacial Maximum. *Nature Geosci* **7**, 662–666 (2014).
47. Svensson, A. et al. A 60 000 year Greenland stratigraphic ice core chronology. *Clim. Past* **4**, 47–57 (2008).
48. Adolphi, F. et al. Connecting the Greenland ice-core and U/Th timescales via cosmogenic radionuclides: Testing the synchronicity of Dansgaard-Oeschger events. *Clim. Past Discuss.* **2018**, 1–39 (2018).
49. Sinnl, G. et al. A multi-ice-core, annual-layer-counted Greenland ice-core chronology for the last 3800 years: GICC21. *Clim. Past* **18**, 1125–1150 (2022).
50. Siegenthaler, U., Heimann, M. & Oeschger, H. ^{14}C variations causd by changes in the global carbon cycle. *Radiocarbon* **22**, 177–191 (1980).
51. McManus, J. F., Francois, R., Gherardi, J.-M., Keigwin, L. D. & Brown-Leger, S. Collapse and rapid resumption of Atlantic meridional circulation linked to deglacial climate changes. *Nature* **428**, 834–837 (2004).
52. Camuera, J. et al. Chronological control and centennial-scale climatic subdivisions of the Last Glacial Termination in the western Mediterranean region. *Quat. Sci. Rev.* **255**, 106814 (2021).
53. Schneider, E. L. Morphological Studies of the Nymphaeaceae. IX. The Seed of Barclaya longifolia Wall. *Botanical Gazette* **139**, 223–230 (1978).
54. Vescovi, E. et al. Interactions between climate and vegetation during the Lateglacial period as recorded by lake and mire sediment archives in Northern Italy and Southern Switzerland. *Quat. Sci. Rev.* **26**, 1650–1669 (2007).
55. Wagner, S., Huth, F., Mohren, F. & Herrmann, I. 1. 5 Silvicultural systems and multiple service forestry. In: *Integrative approaches as an opportunity for the conservation of forest biodiversity* (eds Kraus, D. & Krumm, F.) 64–73 (European Forest Institute, 2013).
56. Monegato, G. et al. Evidence of a two-fold glacial advance during the last glacial maximum in the Tagliamento end moraine system (eastern Alps). *Quat. Res.* **68**, 284–302 (2007).
57. Wick, L. *Late-glacial and early-Holocene palaeoenvironments in Brianza, N Italy*. (na, 1996).
58. Pini, R. et al. Linking North Atlantic and Alpine Last Glacial Maximum climates via a high-resolution pollen-based subarctic forest steppe record. *Quaternary Science Reviews* **294**, 107759 (2022).
59. Clark, J. S. et al. Individual-scale inference to anticipate climate-change vulnerability of biodiversity. *Philos. Trans. R. Soc. B: Biol. Sci.* **367**, 236–246 (2012).
60. Combourieu Nebout, N. et al. Rapid climatic variability in the west Mediterranean during the last 25,000 years from high resolution pollen data. *Clim. Past* **5**, 503–521 (2009).
61. Allard, J. L., Hughes, P. D. & Woodward, J. C. Heinrich Stadial aridity forced Mediterranean-wide glacier retreat in the last cold stage. *Nat. Geosci.* **14**, 197–205 (2021).
62. Rinn F. 2011. TSAP-WinTM Time series analysis and presentation for dendrochronology and related applications. Version 4.64 for Microsoft Windows. User Reference – Heidelberg, Germany, 110pp.
63. Baillie, M. G. & Pilcher, J. R. A simple crossdating program for tree-ring research. *Tree-Ring Bulletin*. **33**, 7–14 (1973).
64. Eckstein, D. & Bauch, J. Beitrag zur Rationalisierung eines dendrochronologischen Verfahrens und zur Analyse seiner Aussagesicherheit. *Forstwissenschaftliches Centralblatt* **88**, 230–250 (1969).
65. Holmes, R. L. Computer-assisted quality control in tree-ring dating and measurement. (1983).
66. Cercatillo, S., Friedrich, M., Kromer, B., Paleček, D. & Talamo, S. Exploring different methods of cellulose extraction for ^{14}C dating. *New J. Chem.* **45**, 8936–8941 (2021).
67. Casella, G. & Robert, C. Monte Carlo statistical methods. University of Florida (2008).
68. Hughen, K. A. & Heaton, T. J. Updated Cariaco basin ^{14}C calibration dataset from 0–60 cal kyr BP. *Radiocarbon*, 1–43, https://doi.org/10.1017/RDC.2020.53 (2020).

Acknowledgements

This research was supported by the European Research Council under the European Union's Horizon 2020 Research and Innovation Programme (grant agreement No. 803147 RESOLUTION, awarded to ST). We thank Leone Fasani for bringing 1994 the first Revine disk to Heidelberg. We thank the major of Revine City, Massimo Magagnin, for his support. We thank Sabine Remmele and Daniel Reichle, Institute of Botany, Hohenheim for help on initial tree-ring measurements and Dr. Helmut Dalitz for helpful support. FA is supported by the Helmholtz Foundation (VG-NG-1501). TJH is funded by UKRI via NE/X009815/1 and EP/X032906/1. We would like to thank the Editor and the three reviewers for their valuable comments that improved considerably the paper.

Author contributions

S.T., B.K., M.F., F.A., and L.W., designed the research. M.F., S.C., D.P., L.T., and E.P., performed the research. S.T., B.K., M.F., F.A., T.J.H., V.T., R.M., and L.W. analyzed data. S.T., B.K., M.F., F.A., and T.J.H., wrote the paper with the contribution of all the co-authors.

Competing interests

The authors declare no competing interests.

Additional information

Supplementary information The online version contains supplementary material available at https://doi.org/10.1038/s43247-023-00929-9.

Correspondence and requests for materials should be addressed to Sahra Talamo, Michael Friedrich, Florian Adolphi or Timothy J. Heaton.

Peer review information *Communications Earth & Environment* thanks David Richards and the other, anonymous, reviewer(s) for their contribution to the peer review of this work. Primary Handling Editors: Joshua Dean and Aliénor Lavergne.